

Bistability in Interstellar Gas-Phase Chemistry

Gai I. Boger and Amiel Sternberg

School of Physics and Astronomy and the Wise Observatory, The Beverly and Raymond Sackler Faculty of Exact Sciences, Tel Aviv University, Ramat Aviv 69978, Israel

amiel@wise.tau.ac.il

ABSTRACT

We present an analysis of “bistability” in gas-phase chemical models of dark interstellar clouds. We identify the chemical mechanisms that allow high- and low-ionization solutions to the chemical rate-equations to coexist. We derive simple analytic scaling relations for the gas densities and ionization rates for which the chemistry becomes bistable. We explain why bistability is sensitive to the H_3^+ dissociative recombination rate coefficient, and why it is damped by gas-grain neutralization.

Subject headings: ISM:molecules – molecular processes

1. Introduction

In this paper we reexamine and analyze the phenomenon of “bistability” that occurs in chemical models of dark interstellar clouds. Bistability was first discussed by Le Bourlot et al. (1993), who found that multiple solutions to the chemical rate-equations sometimes appear in numerical computations of the gas-phase abundances of atomic and molecular species for steady-state dark cloud conditions. When bistability occurs, three sets, rather than a single unique set, of chemical abundances are predicted for identical input cloud parameters such as the total gas density, the cosmic-ray (or X-ray) ionization rate, and the gas-phase supply of heavy elements. Under such circumstances, the solution that is converged to in a numerical simulation, and perhaps, the actual steady-state of a real physical system, depend on the initial conditions and history of the gas.

The subject of bistability begins with Pineau des Forets et al. (1992) who studied how the computed chemical states of dark clouds depend on the gas density and ionization rate. They found, as would be expected, that for a given ionization rate the fractional ionization of the gas decreases roughly as the square-root of the gas density. However, they also

found that the ionization fraction and associated chemical composition changes abruptly, or quasi-discontinuously, at a specific critical transition density. Below the critical density the clouds are in what Pineau des Forets et al. referred to as a “high-ionization” phase (HIP), characterized by high abundances of atomic ions. For densities greater than the critical density the clouds are in a “low-ionization” phase (LIP), with high abundances of molecular ions. Pineau des Forets et al. also identified a chemical instability that, they argued, is responsible for the abrupt transition that they encountered in their calculations. Bistability was subsequently discovered by Le Bourlot et al. (1993) who found that instead of a phase change at a specific critical density, the LIP and HIP “branches” can sometimes overlap for a narrow range of densities. A third (unstable) branch also appears, intermediate between the LIP and HIP solutions.

Further investigations have explored the effects of the assumed gas phase elemental abundances, ionization rates, gas temperatures, chemical reaction rate coefficients, and gas-grain interactions, on the existence and character of the multiple solutions (Le Bourlot et al. 1995ab; Shalabiea & Greenberg 1995; Lee et al. 1998; Pineau des Forets & Roueff 2000; Viti et al. 2001; Charnley & Markwick 2003). These studies have shown that bistability is indeed related to the transition from the HIP to LIP (or vice versa), and that it is sensitive to quantities such as the gas-phase heavy-element abundances (Le Bourlot et al. 1995; Viti et al. 2001), and the adopted chemical network (Lee et al. 1998), including specifically the dissociative recombination rate coefficient of H_3^+ (Pineau des Forets & Roueff 2000). In this paper we explain why the HIP and LIP can overlap, and we identify the chemical mechanisms that allow the possibility of multiple solutions.

We will show that bistability can be simply understood and analyzed using just a handful of reactions. In a nutshell, when bistability occurs atomic ions (usually S^+ ions) are the dominant positive charge carriers for both HIP and LIP conditions. Two modes of neutralization are then available to the gas. In the HIP, neutralization proceeds by slow radiative recombination. In the LIP, neutralization occurs by rapid dissociative recombination, via the formation of intermediate molecular ions in reactions with O_2 molecules (e.g., $\text{S}^+ + \text{O}_2 \rightarrow \text{SO}^+ + \text{O}$). Bistability occurs when a low O_2 abundance in the HIP can be maintained up to maximal gas densities that are *greater* than the minimal densities above which a large O_2 density is maintained in the LIP. We will show by means of a simple analysis why this is possible. The explanation involves a chemical instability, of a type first introduced by Pineau des Forets et al. (1992), but not given sufficient attention in subsequent studies.

Bistability may be of primarily theoretical interest since, as we will discuss, it is a purely gas-phase chemical effect. If realistic gas-dust neutralization processes are included, the multiple solutions are damped or eliminated entirely (cf. Shalabiea & Greenberg 1995).

We will illustrate this by considering the effect of grain-assisted ion-electron recombination (Weingartner & Draine 2001) on the chemistry. Nevertheless, because bistability has been the subject of considerable discussion in the literature, we feel that a fresh analysis of how, why, and when it occurs is warranted.

The plan of our paper is as follows. In §2 we present results of an illustrative numerical computation in which bistability occurs. In §3 we discuss the key chemical instability that drives the steady-state solutions to either the LIP or HIP. In §4 we derive simple analytic formulae that show how the range of gas densities and ionization rates for which the gas becomes bistable depends on the elemental abundances and several important chemical rate coefficients. In §5 we analyze the sensitivity of bistability to the H_3^+ dissociative recombination rate coefficient. In §6 we explain why gas-grain neutralization processes damp and eliminate bistability. We summarize in §7.

2. Computations

We first illustrate the phenomenon of bistability in a detailed numerical computation. For this purpose we calculate the steady-state atomic and molecular abundances for dark cloud conditions, as functions of the gas density. We include only gas-phase formation and destruction processes, except for molecular hydrogen (H_2), which we assume is formed on grain surfaces. The chemistry is driven by cosmic-ray impact ionization of hydrogen and helium, followed by standard sequences of ion-molecule, charge-exchange, and neutral-neutral reactions. The chemistry is also mediated by radiative and dissociative recombination, and cosmic-ray induced photoionization and photodissociation. The effects of externally incident FUV photons are excluded.

We use the Boger & Sternberg (2005) network for a system consisting of 70 atomic and molecular carbon, nitrogen, oxygen, sulfur, and silicon bearing species (see also Sternberg & Dalgarno 1995). We neglect all other heavy elements. Our set of 868 reactions and rate coefficients is based mainly on the UMIST99 compilation (Le Teuff et al. 2000) with some modifications and alterations¹. As in Boger & Sternberg (2005) we adopt ζ *Oph* gas-phase abundances, with $\text{C}/\text{H}=1.32 \times 10^{-4}$ (Cardelli et al. 1993), $\text{N}/\text{H}=7.50 \times 10^{-5}$ (Meyer et al. 1997), $\text{O}/\text{H}=2.84 \times 10^{-4}$ (Meyer et al. 1998), $\text{Si}/\text{H}=1.78 \times 10^{-6}$ (Cardelli et al. 1994), and $\text{S}/\text{H}=8.30 \times 10^{-6}$ (Lepp et al. 1988). We set $\text{He}/\text{H}=0.1$. We assume a constant gas temperature of $T = 50$ K for the entire range of gas densities that we consider.

¹Our input list of rate coefficients is available at <ftp://wise3.tau.ac.il/pub/amiel/pdr>.

In our calculations we solve the equations of chemical equilibrium

$$\sum_{jl} k_{ijl}(T)n_jn_l + \sum_j \xi_{ij}n_j = n_i \left\{ \sum_{jl} k_{jil}n_l + \sum_j \xi_{ji} \right\} \quad (1)$$

for the densities n_i of all species i in our set. In these equations, $k_{ijl}(T)$ are the temperature-dependent rate coefficients ($\text{cm}^3 \text{s}^{-1}$) for chemical reactions between species j and l that lead to the production of i , and ξ_{ij} are the cosmic-ray destruction rates (s^{-1}) of species j with products i . The parameters ξ_{ij} include impact ionizations of hydrogen and helium by the cosmic-ray protons and secondary electrons, as well as photo-destruction of heavy atomic and molecular species by induced UV photons. The ξ_{ij} are all proportional to $\zeta \equiv 10^{-17}\zeta_{-17} \text{s}^{-1}$, the cosmic-ray ionization rate of molecular hydrogen (Sternberg et al. 1987; Gredel et al. 1989)

The densities n_i must also satisfy the supplementary equations of element and charge conservation. These are,

$$\sum_i \alpha_{im}n_i = X_m n_{\text{tot}} \quad (2)$$

where α_{im} is the number of atoms of element m contained in species i , X_m is the total abundance of element m relative to the total density n_{tot} of hydrogen nuclei, and

$$\sum_i q_i n_i = 0 \quad (3)$$

where q_i is the charge of species i . In our computations, the negative charge is carried entirely by free electrons.

H_2 molecules are formed primarily on dust grains and are destroyed by cosmic-ray ionization. A separate equation may then be written for the H/H_2 balance,

$$\zeta n_{\text{H}_2} = R n_{\text{tot}} n_{\text{H}} \quad (4)$$

where n_{H} and n_{H_2} are the atomic and molecular hydrogen densities respectively, and $R = 3 \times 10^{-18} T^{1/2} \text{ cm}^3 \text{ s}^{-1}$ is the H_2 grain surface formation rate coefficient (Biham et al. 2002; Vidali et al. 2004).

For fixed gas temperature and gas-phase elemental abundances, the density fractions $x_i \equiv n_i/n_{\text{tot}}$ as determined by equations (1)-(4) depend on the single parameter n_{tot}/ζ (e.g., Lepp & Dalgarno 1996; Lee et al. 1998), as is readily seen by dividing each term in these equations by n_{tot}^2 . We consider a range of parameters for which almost all of the hydrogen is in the form of H_2 , so that $n_{\text{tot}} = 2n_{\text{H}_2}$. We therefore present our results as functions of the ratio $n_{\text{H}_2}/\zeta_{-17}$ (cm^{-3}).

We solve equations (1)-(4) numerically via Newton-Raphson (NR) iteration. In our procedure we vary the density along the HIP and LIP branches and use the solutions from the previous density step as the “initial guess” for the NR iteration in the next density step. In the bistability region we carry out repeated NR iterations with random initial guesses, so that all three branches are found.

In Figure 1 we plot the densities n_i/ζ_{-17} , and density fractions n_i/n_{H_2} , as functions of $n_{\text{H}_2}/\zeta_{-17}$ ranging from 10^2 to 10^4 cm^{-3} , for several species of interest. Panels (a) and (b) display our results for electrons, C^+ , S^+ , H_3^+ , and a sum over all molecular ions. Panels (c) and (d) display our results for the neutral species C, O, CO and O_2 . Several important features are apparent in Figure 1, some of which have been noted in previous discussions.

For our assumed elemental abundances and gas temperature, a high-ionization phase (HIP) is present for densities less than $(n_{\text{H}_2}/\zeta_{-17})_{\text{max}} = 675 \text{ cm}^{-3}$, and a low-ionization phase (LIP) is present for densities greater than $(n_{\text{H}_2}/\zeta_{-17})_{\text{min}} = 370 \text{ cm}^{-3}$. The HIP and LIP overlap, and the gas is bistable, between these minimal and maximal densities. The HIP and LIP solutions are connected by a third branch that we refer to here as the MIX solution.

In the HIP, the positive charge is carried entirely by atomic ions. S^+ is the dominant ion down to $n_{\text{H}_2}/\zeta_{-17} = 60 \text{ cm}^{-3}$. At lower densities C^+ takes over, and for $n_{\text{H}_2}/\zeta_{-17} < 1.1 \text{ cm}^{-3}$, H^+ dominates. In the LIP, the molecular ions HCO^+ and H_3O^+ are the primary positive charge carriers for densities greater than $n_{\text{H}_2}/\zeta_{-17} > 6 \times 10^3 \text{ cm}^{-3}$. However, S^+ dominates at lower densities in the LIP. Most importantly, in our calculation S^+ is the primary positive charge carrier in *both* the HIP and LIP for the densities at which bistability occurs.

The fractional ionization increases from a minimum value $x_e = 6 \times 10^{-6}$ as the density decreases from $(n_{\text{H}_2}/\zeta_{-17})_{\text{max}}$ in the HIP. In the LIP, the fractional ionization decreases from a maximum value of $x_e = 2 \times 10^{-6}$ as the density increases from $(n_{\text{H}_2}/\zeta_{-17})_{\text{min}}$. The fractional ionization drops by a factor of ~ 10 in moving from the HIP to LIP in the bistability region.

The free atomic carbon density and the C/CO abundance ratio is large in the HIP. The ratio $\text{C}/\text{CO} \approx 0.3$ in the bistability region, and exceeds unity for $n_{\text{H}_2}/\zeta_{-17} \lesssim 55 \text{ cm}^{-3}$. In the LIP the C density and the C/CO ratio are small. In our computation the C/CO ratio drops by a factor ~ 50 in moving from the HIP to the LIP. The drop in C/CO is associated with an *increase* in the O_2 density and the O_2/CO ratio. It is very significant that the C and O_2 densities vary in opposite directions in the transition between the HIP and LIP.

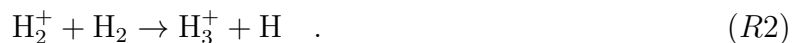
On the MIX branch the fractional ionization, and the C/CO and O_2/CO ratios, are intermediate between the HIP and LIP. S^+ is also the dominant positive ion on the MIX branch. However, the fractional ionization increases with gas density along the MIX.

In Table 1 we list the densities of selected atomic and molecular species for the three HIP, LIP, and MIX solutions, for $n_{\text{H}_2} = 4.3 \times 10^2 \text{ cm}^{-3}$ and $\zeta = 1.0 \times 10^{-17} \text{ s}^{-1}$. We also list the HIP/LIP density ratios for these values of n_{H_2} and ζ . Atomic ions, e.g., S^+ , Si^+ , and C^+ , are abundant in the HIP solution. In the LIP solution, molecular ions such as H_3^+ , HCO^+ , and H_3O^+ are abundant, leading to more OH, H_2O , and O_2 than in the HIP. The oxygen bearing molecules, NO, SO, and SiO, are enhanced by the large O_2 density that is maintained in the LIP. Carbon bearing molecules, such as CN and HCN, are enhanced in the HIP because of the large atomic carbon density in this phase (see also Boger & Sternberg 2005). CS is produced by reactions of SO (enhanced in the LIP) with C (enhanced in the HIP) so that the CS density changes by only a factor of ~ 2 in moving from the LIP and HIP.

3. Chemistry and Instability

Figure 1 shows that as the gas density n_{H_2} is increased along the sequence of HIP solutions an abrupt jump to the LIP branch occurs when n_{H_2} rises above $(n_{\text{H}_2}/\zeta_{-17})_{\text{max}}$. Similarly, as n_{H_2} is decreased along the LIP, a jump to the HIP occurs when n_{H_2} falls below $(n_{\text{H}_2}/\zeta_{-17})_{\text{min}}$. As we now discuss, these jumps are signatures of a simple chemical instability involving electrons, S^+ and H_3^+ ions, C atoms, and O_2 molecules. The instability can be understood by considering the gas-phase formation and destruction sequences for these species, for gas densities where the bistable solutions occur. We first discuss the HIP and LIP, and we then consider the MIX.

We begin with H_3^+ . In both the HIP and LIP, this ion is formed by cosmic-ray ionization of H_2 followed by proton transfer,



In the HIP, the electron fraction is large, and dissociative recombination

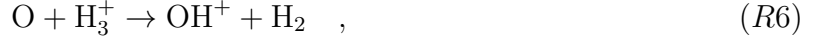


dominates the removal of the H_3^+ . However, in the LIP the electron fraction is small, and the H_3^+ is removed by

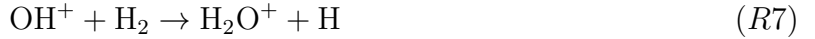


For a gas temperature of 50 K, dissociative recombination dominates the destruction of H_3^+ when $n(e)/n(\text{CO}) > 10^{-2}$.

In both the HIP and LIP, the production of O_2 is initiated by proton transfer



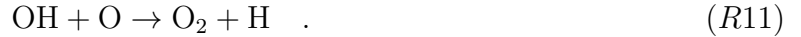
which is followed by abstraction



dissociative recombination



and the neutral-neutral reaction



However, the O_2 is destroyed in different ways in the two phases. In the HIP, the density of free atomic carbon is large, and the O_2 is removed by



In the LIP, the C density is small, and the O_2 is removed much less efficiently in reactions with less abundant atoms and atomic ions. An upper limit on the O_2 density in the LIP is set by cosmic-ray induced photodissociation



Reaction (R13) is inefficient, and the O_2 density becomes large in the LIP.

In the HIP, C^+ is produced by cosmic-ray driven helium impact ionization of CO,



This is then followed by rapid charge transfer



which leads to the production of S^+ and C. The S^+ ions are removed by radiative recombination,



The C atoms are removed by cosmic-ray induced photoionization



Because cosmic-ray photoionization is inefficient, a large C density is maintained in the HIP.

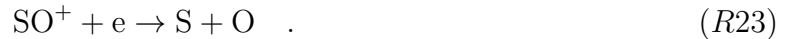
In the LIP, C^+ is also produced by helium impact ionization ([R14] and [R15]). However, because the O_2 density is large in the LIP, the C^+ ions are rapidly neutralized by the sequence



and the C^+ density becomes small. In the LIP, charge transfer between C^+ and S ([R16]) contributes negligibly to the removal of C^+ , or to the formation of S^+ . The main source of S^+ in the LIP is cosmic-ray induced photoionization



Crucially, O_2 also dominates the neutralization of S^+ in the LIP, via



For a gas temperature of 50 K, neutralization of S^+ by O_2 dominates over radiative recombination when $n(O_2)/n(e) > 0.8$. Finally, the C atoms formed by (R20) are also removed by reactions with O_2 ([R12]), and the C density becomes small in the LIP.

For the gas densities of interest, most of the gas-phase sulfur is present as S and S^+ in both the HIP and LIP, with only a small fraction bound in molecules. S^+ is the primary positive charge carrier in both the HIP and LIP. However, in the HIP S^+ is removed by radiative recombination, whereas in the LIP by reactions with O_2 . In the HIP, H_3^+ is removed by dissociative recombination, C is removed by cosmic-ray induced photoionization, and O_2 is removed by C. In the LIP, H_3^+ is removed by CO, C is removed by O_2 , and O_2 is limited by cosmic-ray induced photodissociation. The abundance ratio C/ O_2 is large in the HIP, and is small in the LIP.

Now consider a gas where S^+ is again the dominant charge carrier, but which differs from the HIP or LIP in that dissociative recombination contributes significantly to the removal

of H_3^+ (as in the HIP), while on the other hand S^+ is neutralized by O_2 (as in the LIP). Assume also that O_2 is produced by the sequence (R6)-(R11), and that the O_2 destruction rate increases if the O_2 density decreases. This is possible when reaction (R12) between O_2 and C is the dominant destruction mechanism for both species, so that $n(\text{C})$ increases if $n(\text{O}_2)$ decreases. For these conditions a chemical instability can occur, as we demonstrate with the following perturbation analysis.

Consider a possible solution to the steady-state rate equations. With the above assumptions this requires $n(e) = n(\text{S}^+)$. Now consider a perturbative increase in the ionization fraction $x_e \equiv n(e)/n_{\text{H}_2}$, carried out at fixed gas density n_{H_2} . This will reduce H_3^+ by a factor that depends on the relative efficiencies of dissociative recombination versus reaction with CO in removing the H_3^+ . The O_2 is removed by C (via [R12]), so for a given C density the reduction in H_3^+ will lead to an equal reduction in O_2 (since O_2 is formed by [R6]-[R11])². However, the decrease in O_2 will lead to an increase in C, since the C is removed by O_2 (again via [R12]). This reduces O_2 further still. The S^+ density then increases by a factor equal to the total reduction in O_2 (since S^+ is removed by O_2). Finally, to close the loop, $n(e)$ must then be set equal to the new value of $n(\text{S}^+)$, since by assumption S^+ carries the positive charge. However, if the increase in S^+ is larger than the initial increase in the electron density the cycle “runs away” in a positive feedback loop.

This H_3^+ - O_2 - S^+ cycle is illustrated schematically in Figure 2. It is clear that the cycle can also lead to a run-away decrease in the electron density, in response to a perturbative decrease in $n(e)$. For increasing electron densities, O_2 decreases and C increases. For decreasing electron densities, O_2 increases and C decreases.

The instability shuts off for sufficiently large or small fractional ionizations. For large x_e , radiative recombination, rather than removal by O_2 , becomes the dominant S^+ neutralization process. For small x_e , reaction with CO replaces dissociative recombination as the H_3^+ removal mechanism. Either way, the H_3^+ - O_2 - S^+ instability cycle shuts off, and the gas becomes chemically stable.

In the HIP, dissociative recombination dominates the destruction of H_3^+ , but S^+ is removed by radiative recombination. In the LIP, S^+ is removed by O_2 , but H_3^+ is removed by CO. Crucially therefore, the H_3^+ - O_2 - S^+ cycle is inoperative on the HIP and LIP branches, and these solutions are chemically stable.

We now identify the maximum possible density for the HIP, $(n_{\text{H}_2}/\zeta_{-17})_{\text{max}}$, as the point at which O_2 , *as formed and destroyed in the HIP*, becomes sufficiently abundant to begin

²In this analysis we assume that most of the oxygen not locked in CO remains atomic.

removing the S^+ . When this occurs, the $H_3^+-O_2-S^+$ cycle turns on (since H_3^+ is still being removed by electrons) and a stable HIP is no longer possible. As the density is increased above $(n_{H_2}/\zeta_{-17})_{\max}$ the instability induces a sharp drop in $n(e)$. As the electron density drops in the run-away loop, O_2 increases and C decreases. The system is finally stabilized when the electron density becomes sufficiently small for reactions with CO to begin dominating the removal of H_3^+ . The $H_3^+-O_2-S^+$ cycle then turns off, and a stable solution on the LIP is reached.

Similarly, we identify the minimum possible density for the LIP, $(n_{H_2}/\zeta_{-17})_{\min}$, as the point at which the fractional ionization, *as determined for the LIP*, becomes sufficiently large for dissociative recombination to begin dominating the removal of H_3^+ . When this occurs, the $H_3^+-O_2-S^+$ cycle turns on, (since S^+ is still removed by O_2) and a stable LIP is no longer possible. As the density is decreased below $(n_{H_2}/\zeta_{-17})_{\min}$ the instability induces a sharp rise in $n(e)$. As the electron density increases, O_2 decreases and C increases. The electron density rises until it becomes sufficiently large (and the O_2 density sufficiently small) for radiative recombination to dominate the neutralization of S^+ . The instability then shuts off, and a stable solution on the HIP is reached.

The MIX branch can now also be understood. It represents the locus of equilibrium solutions, with varying n_{H_2} , for which the $H_3^+-O_2-S^+$ cycle *is* operative, but for which any change in electron density is precisely matched by a corresponding change in the S^+ density. For these solutions, dissociative recombination and reactions with CO both contribute to the removal of H_3^+ , and S^+ is removed by O_2 . Furthermore, reaction (R12) is the dominant destruction mechanism, for both O_2 and C . As the electron fraction increases along the MIX, the O_2 formation rate decreases, but by a factor that is smaller than the increase in electron density. The density of C atoms (which remove the O_2) increases such that the total increase in O_2 , and the resulting increase in S^+ , exactly matches the increase in electron density.

Figure 3 summarizes the key characteristics of the HIP, LIP, and MIX branches, as described above. The triangular symbols indicate the three “legs” of the $H_3^+-O_2-S^+$ cycle illustrated in Figure 2. In the HIP, removal of S^+ by O_2 is inoperative so this leg is labeled as “OFF”. In the LIP, dissociative recombination of H_3^+ is inoperative so this leg is “OFF” for this phase. For the MIX, which shares properties of both the HIP and LIP, all three legs of the $H_3^+-O_2-S^+$ cycle operate, and are “ON”. In Figure 3 we also indicate the dominant removal reactions for S^+ , H_3^+ , O_2 , and C , for each of the three branches.

The HIP and LIP as originally defined by Pineau des Forets et al. (1992), were distinguished by whether H_3^+ is removed by dissociative recombination (HIP), or by reactions

with CO (LIP)³. Here we have identified a second, and crucial, distinction. In the HIP, atomic ions, are removed by (slow) radiative recombination. In the LIP the atomic ions are effectively removed by rapid dissociative recombination, via the formation of intermediate molecular ions, as in the sequence (R22) and (R23).

In our discussion it is S^+ that plays the crucial role of positive charge carrier in both the HIP and LIP. The reason why simultaneous HIP, LIP, and MIX solutions are possible now emerges. Bistability occurs when radiative recombination is able to dominate the removal of S^+ in the HIP up to maximal gas densities that are *greater* than the minimal densities down to which reactions with CO dominate the removal of H_3^+ in the LIP. Alternatively, bistability occurs when it is possible for a low HIP O_2 abundance to be maintained up to maximal gas densities that are greater than the minimal gas densities down to which a large LIP O_2 density can be maintained. This is our key result. When this occurs, there exists a range of densities for which the S^+ ions are either removed slowly via radiative recombination (HIP, low O_2) or rapidly via dissociative recombination (LIP, high O_2). The simultaneous solutions are separated by the $H_3^+ - O_2 - S^+$ instability cycle, which drives the O_2 density to either small (HIP) or large (LIP) values.

The critical densities $(n_{H_2}/\zeta_{-17})_{\min}$ and $(n_{H_2}/\zeta_{-17})_{\max}$, as defined above, depend on a variety of factors including the elemental abundances, and several specific chemical rate coefficients. In §4 we derive simple analytic expressions for these critical densities. We determine, analytically, when it is possible for $(n_{H_2}/\zeta_{-17})_{\max}$ to exceed $(n_{H_2}/\zeta_{-17})_{\min}$, which is our condition for bistability, and we determine the range of gas densities for which bistability occurs.

4. Analysis

4.1. HIP and n_{\max}

For stable HIP conditions the electron density must be sufficiently large for dissociative recombination to dominate the removal of H_3^+ , and the O_2 density must be sufficiently small for radiative recombination to dominate the removal of S^+ . We now show analytically that consistent solutions that satisfy these HIP conditions are possible provided the density is less than a critical *maximum* gas density.

³These authors also recognized that the transition from the LIP to HIP is driven by a chemical instability involving O_2 . However, they did not consider how the instability is quenched in each phase.

We first derive an expression for the O_2 density in the low density limit of the HIP. We show that in this limit the O_2 density is small, and radiative recombination dominates the removal of S^+ . We then show that our low density expression for O_2 remains consistent only up to a maximal gas density. We identify this as the maximum possible density for HIP solutions. We then verify that dissociative recombination dominates the removal of H_3^+ , a necessary condition for the HIP, for all densities below this critical density.

In the HIP, O_2 is produced by the sequence (R6)-(R11), and is removed by reaction (R12) with atomic carbon. This gives,

$$n(O_2) = \frac{n(H_3^+)n(O)k_6d_{OH}}{n(C)k_{12}} \quad (5)$$

where $k_6 = 8.0 \times 10^{-10}$ and $k_{12} = 3.3 \times 10^{-11} \text{ cm}^3 \text{ s}^{-1}$ are the rate coefficients (at 50 K) of (R6) and (R12), and $d_{OH} = 0.74$ is the fraction (Jensen et al. 2000) of H_3O^+ recombinations that produce OH. Atomic carbon is produced by helium impact ionization of CO followed by immediate charge transfer neutralization ([R15] and [R16]), and is removed by cosmic-ray induced photoionization ([R18]). Because (R15) dominates the removal of He^+ , the rate of C formation equals the cosmic-ray ionization rate of helium. Therefore,

$$\frac{n(C)}{n_{H_2}} = \frac{X_{He}}{p_{18}} = 10^{-4} \quad , \quad (6)$$

independent of n_{H_2}/ζ . In this expression $p_{18} = 1.02 \times 10^3$ is the efficiency of (R18), and $X_{He} = 0.1$ is the helium abundance. It is clear that a large C density is indeed expected in the HIP, since $n(C)/n_{H_2} = 10^{-4}$ is comparable to the typical total gas-phase carbon abundance (e.g. $X_C = 1.32 \times 10^{-4}$ in our numerical model). The large C density keeps the O_2 abundance small in the HIP.

The O_2 density is proportional to H_3^+ , which in turn, depends on the electron density. For electrons we set $n(e) = n(S^+)$. The S^+ is produced the same way as atomic carbon, i.e., by helium impact ionization of CO followed by charge transfer ([R15] and [R16]). We assume that the S^+ is removed by radiative recombination. This gives,

$$x_e \equiv \frac{n(e)}{n_{H_2}} = \left(\frac{X_{He}\zeta}{k_{17}n_{H_2}} \right)^{1/2} = 2.9 \times 10^{-4} \left(\frac{\zeta_{-17}}{n_{H_2}} \right)^{1/2} \quad . \quad (7)$$

where the radiative recombination rate coefficient $k_{17} = 1.2 \times 10^{-11} \text{ cm}^3 \text{ s}^{-1}$. In this limit the fractional ionization varies as $(n_{H_2}/\zeta)^{-1/2}$. For $n_{H_2}/\zeta_{-17} = 100 \text{ cm}^{-3}$, equation (7) gives $x_e = 2.9 \times 10^{-5}$ in good agreement with 2.3×10^{-5} computed numerically (see Figure 1).

H_3^+ is produced by cosmic-ray ionization and is removed by dissociative recombination, so that

$$\frac{n(H_3^+)}{n_{H_2}} = \frac{\zeta}{k_{3,4}n(e)} = \frac{1}{k_{3,4}} \left(\frac{k_{17}\zeta}{X_{He}n_{H_2}} \right)^{1/2} = 2.0 \times 10^{-7} \left(\frac{\zeta_{-17}}{n_{H_2}} \right)^{1/2} \quad (8)$$

where $k_{3,4} = 1.7 \times 10^{-7} \text{ cm}^3 \text{ s}^{-1}$ is the total rate coefficient for dissociative recombination. The H_3^+ abundance also varies as $(n_{\text{H}_2}/\zeta)^{-1/2}$. For $n_{\text{H}_2}/\zeta_{-17} = 100 \text{ cm}^{-3}$, equation (8) gives $n(\text{H}_3^+)/n_{\text{H}_2} = 2.0 \times 10^{-8}$, as also computed numerically.

Inserting equations (6), (7), and (8) into equation (5) gives

$$\frac{n(\text{O}_2)}{n_{\text{H}_2}} = \frac{2X'_\text{O}}{X_{\text{He}}^{3/2}} \frac{k_{17}^{1/2}}{k_{12}} \frac{k_6}{k_{3,4}} d_{\text{OHP}18} \left(\frac{\zeta}{n_{\text{H}_2}} \right)^{1/2} = 1.1 \times 10^{-5} \left(\frac{\zeta_{-17}}{n_{\text{H}_2}} \right)^{1/2} \quad (9)$$

where $X'_\text{O} \equiv X_\text{O} - X_\text{C} = 1.5 \times 10^{-4}$, and where we have assumed that most of the oxygen not bound in CO remains atomic. The O_2 abundance varies as $(n_{\text{H}_2}/\zeta)^{-1/2}$. For $n_{\text{H}_2}/\zeta_{-17} = 100 \text{ cm}^{-3}$, equation (9) gives $n(\text{O}_2)/n_{\text{H}_2} = 1.1 \times 10^{-6}$, close to 3.0×10^{-7} computed numerically.

The O_2 density as given by equation (9), is sufficiently small for removal of S^+ by O_2 to be negligible compared to radiative recombination. This can be seen by considering the ratio of the S^+ removal rates

$$\frac{k_{22}n(\text{O}_2)}{k_{17}n(\text{e})} = \frac{2X'_\text{O}}{X_{\text{He}}^2} \frac{k_6 k_{22}}{k_{3,4} k_{12}} d_{\text{OHP}18} = 0.05 \quad (10)$$

where $k_{22} = 1.5 \times 10^{-11} \text{ cm}^3 \text{ s}^{-1}$ is the rate coefficient for reaction (R22). Because this ratio is independent of n_{H_2}/ζ , the removal of S^+ by O_2 is negligible at all densities so long as equation (9) for the O_2 abundance is an appropriate approximation.

Equation (9) is valid so long as cosmic-ray photons dominate the removal of the carbon atoms, so that the C density is given by equation (6). However, cosmic-ray induced destruction occurs at a rate independent of n_{H_2} , whereas the O_2 density as given by equation (9) varies as $n_{\text{H}_2}^{1/2}$. Therefore, for sufficiently large n_{H_2} reactions with O_2 ([R12]) must eventually dominate the removal of the C atoms. When this occurs the C density becomes small, and the O_2 density must become large (see equation [5]). We identify this as the point where O_2 becomes sufficiently abundant to begin removing the S^+ . However, because H_3^+ continues to be removed by dissociative recombination, the H_3^+ - O_2 - S^+ instability cycle turns on at this point, and a stable HIP is no longer possible.

Thus, the HIP can be maintained so long as the O_2 density given by equation (9) is small enough for cosmic-ray photoionization to dominate the removal of the C atoms. This condition,

$$\frac{k_{12}n(\text{O}_2)}{p_{18}\zeta} = \frac{2X'_\text{O}}{X_{\text{He}}^{3/2}} \frac{k_6}{k_{3,4}} k_{17}^{1/2} d_{\text{OH}} \left(\frac{n_{\text{H}_2}}{\zeta} \right)^{1/2} < 1 \quad (11)$$

provides a maximal density for HIP solutions. For our standard elemental abundances and rate-coefficients

$$\left(\frac{n_{\text{H}_2}}{\zeta_{-17}} \right)_{\text{max}} = 7.63 \times 10^2 \text{ cm}^{-3} \quad (12)$$

This is slightly larger than our numerically computed density of 675 cm^{-3} at which the transition to the LIP occurs (see Figure 1).

For consistency we must verify that dissociative recombination dominates the removal of H_3^+ for densities as high as $(n_{\text{H}_2}/\zeta)_{\text{max}}$. Dissociative recombination dominates when the ratio

$$\frac{k_{3,4}n(e)}{k_5n(\text{CO})} = \left(\frac{X_{\text{He}}}{k_{17}}\right)^{1/2} \frac{k_{3,4}}{k_5} \frac{1}{X_{\text{C}}} \left(\frac{\zeta}{n_{\text{H}_2}}\right)^{1/2} \gg 1 \quad , \quad (13)$$

where $k_5 = 1.7 \times 10^{-9} \text{ cm}^3 \text{ s}^{-1}$ is the rate coefficient of reaction (R5). For $(n/\zeta_{-17})_{\text{max}} = 7.63 \times 10^2 \text{ cm}^{-3}$ this ratio equals 8.0, so consistency is obtained.

4.2. LIP and n_{min}

In the LIP, the electron density must be sufficiently small for CO to dominate the removal of H_3^+ , and the O_2 density must be sufficiently large for O_2 to dominate the removal of S^+ . We now show that these conditions can be satisfied, provided the gas density is greater than a critical *minimum* density.

To show this, we first derive an expression for the electron density assuming that S^+ is removed by abundant O_2 , with an upper limit for the O_2 density set by cosmic-ray induced photodissociation. We show that CO then dominates the removal of H_3^+ for densities greater than a minimum critical density. We then verify that the assumption that O_2 dominates the removal of S^+ is consistent for densities greater than this critical density.

For the electron density in the LIP we again assume that $n(e) = n(\text{S}^+)$. In the LIP, S^+ is produced by cosmic-ray induced photoionization, and we assume that it is removed by O_2 . This gives,

$$\frac{n(e)}{n_{\text{H}_2}} = \frac{2X_{\text{S}}p_{21}\zeta}{k_{22}n(\text{O}_2)} \quad (14)$$

where $p_{21} = 2.0 \times 10^3$ is the efficiency of (R21). H_3^+ is removed by CO, so that

$$\frac{n(\text{H}_3^+)}{n_{\text{H}_2}} = \frac{\zeta}{k_5n(\text{CO})} = \frac{1}{2k_5X_{\text{C}}} \frac{\zeta}{n_{\text{H}_2}} = 2.2 \times 10^{-5} \frac{\zeta_{-17}}{n_{\text{H}_2}} \quad , \quad (15)$$

where we have assumed that in the LIP all of the carbon is locked in CO. For $n_{\text{H}_2}/\zeta_{-17} = 10^3$, equation (14) gives $n_{\text{H}_3^+}/n_{\text{H}_2} = 2.2 \times 10^{-8}$, in good agreement with the numerically computed 1.0×10^{-8} .

For O_2 we again assume the production sequence (R6)-(R11). If the O_2 is removed by

only cosmic-ray induced photodissociation,

$$\frac{n(\text{O}_2)}{n_{\text{H}_2}} = \frac{n(\text{H}_3^+)n(\text{O})k_6d_{\text{OH}}}{\zeta p_{13}n_{\text{H}_2}} = \frac{k_6}{k_5} \frac{1}{p_{13}} d_{\text{OH}} \frac{X'_\text{O}}{X_\text{C}} = 2.3 \times 10^{-4} \quad , \quad (16)$$

where $p_{13} = 1.7 \times 10^3$ is the efficiency of (R13). This is actually an upper-limit for the O_2 abundance because additional chemical reactions contribute to the removal of the O_2 in the LIP. In this approximation the O_2 density is independent of n_{H_2}/ζ , consistent with our numerical computations (see Figure 1). Because the upper limit is close to the total available oxygen not locked in CO, we set $n(\text{O}_2)/n_{\text{H}_2} \equiv 2f_{\text{O}_2}X'_\text{O}$, where the O_2 fraction $f_{\text{O}_2} \lesssim 1$. In our numerical computation $f_{\text{O}_2} \approx 0.2$ (see Figure 1).

The electron fraction, x_e , is then

$$\frac{n(\text{e})}{n_{\text{H}_2}} = \frac{X_\text{S} p_{21}}{X'_\text{O} k_{22} f_{\text{O}_2} n_{\text{H}_2}} \frac{1}{\zeta} = 7.4 \times 10^{-5} \frac{1}{f_{\text{O}_2}} \frac{\zeta_{-17}}{n_{\text{H}_2}} \quad . \quad (17)$$

In this limit x_e varies as $(n_{\text{H}_2}/\zeta)^{-1}$. For $f_{\text{O}_2} = 0.2$, equation (17) gives $x_e = 3.7 \times 10^{-7}$, in good agreement with 4.1×10^{-7} in Figure 1.

The electron density as given by equation (17) is independent of n_{H_2} , whereas the CO density decreases with n_{H_2} . Reactions with CO can therefore dominate the removal of H_3^+ only down to a minimal density set by the condition

$$\frac{k_5 n(\text{CO})}{k_{3,4} n(\text{e})} = \frac{2X_\text{C}X'_\text{O}}{X_\text{S}} \frac{k_5 k_{22}}{k_{3,4} p_{21}} f_{\text{O}_2} \frac{n_{\text{H}_2}}{\zeta} > 1 \quad . \quad (18)$$

This relation provides a minimal critical density

$$\left(\frac{n_{\text{H}_2}}{\zeta_{-17}} \right)_{\text{min}} = \frac{28}{f_{\text{O}_2}} \text{ cm}^{-3} \quad (19)$$

for which LIP solutions are possible. For $f_{\text{O}_2} = 0.2$, this is slightly smaller than the numerically computed value of 370 cm^{-3} at which the transition from the LIP to HIP occurs (see Figure 1). When the gas density falls below the critical density electrons remove H_3^+ , but O_2 continue to remove S^+ . The $\text{H}_3^+ - \text{O}_2 - \text{S}^+$ instability cycle therefore turns on, and the gas is driven from the LIP to the HIP.

For consistency we must now verify that reactions with O_2 dominate the removal of S^+ everywhere in the LIP. This requires that

$$\frac{k_{22}n(\text{O}_2)}{k_{17}n(\text{e})} = \frac{2X'_\text{O}{}^2}{X_\text{S}} \frac{k_{22}^2}{k_{17}p_{21}} f_{\text{O}_2}^2 \frac{n_{\text{H}_2}}{\zeta} = 5.1 f_{\text{O}_2}^2 \frac{n_{\text{H}_2}}{\zeta_{-17}} \gg 1 \quad . \quad (20)$$

for all LIP densities, down to the minimal density. Inserting $(n/\zeta_{-17})_{\text{min}}$ as given by equation (19) gives $k_{22}n(\text{O}_2)/k_{17}n(\text{e}) = 142f_{\text{O}_2}$. We conclude that consistent LIP solutions are obtained even for f_{O_2} as small as ~ 0.01 (for which the O_2 density in the LIP is still much larger than in the HIP.)

5. Scaling

The key result of the above analysis is that for our standard parameters $(n/\zeta_{-17})_{\max}$, as given by equation (12), is *greater* than $(n/\zeta_{-17})_{\min}$, as given by equation (19). The gas is therefore bistable between the maximal HIP density and minimum LIP density. The MIX branch must therefore “switch back” from the maximal HIP density to the minimal LIP density. The $\text{H}_3^+\text{-O}_2\text{-S}^+$ instability cycle drives the O_2 density to either very low values in the HIP where a large ionization fraction is maintained by slow radiative recombination, or it drives the O_2 density to very large values in the LIP where a low ionization fraction is maintained by rapid dissociative recombination. Our analytic estimates for the two critical densities are in good agreement with the numerical results displayed in Figure 1.

Equations (11) and (18) show that the critical densities depend on several parameters, including the gas-phase elemental abundances of carbon, oxygen, sulfur and helium, and on several specific chemical rate coefficients, including $k_{3,4}$, the dissociative recombination rate coefficient of H_3^+ . Varying any of these parameters alters the range of densities for which bistability occurs, or eliminates it entirely if $(n/\zeta_{-17})_{\max}$ becomes smaller than $(n/\zeta_{-17})_{\min}$.

A dependence of bistability on $k_{3,4}$, a rate coefficient that has been the subject of much investigation and controversy (see e.g., McCall et al. 2004), was found in numerical computations by Pineau des Forets & Roueff (2000). In their calculations (see their Fig. 4) they set $n_{\text{H}_2}/\zeta_{-17} = 2.5 \times 10^3 \text{ cm}^{-3}$, and varied $k_{3,4}$ from 10^{-8} to $10^{-6} \text{ cm}^3 \text{ s}^{-1}$. They found that the gas is in the LIP or HIP, for low or high values of $k_{3,4}$, and that it is bistable for intermediate H_3^+ recombination efficiencies. Our analysis provides an explanation for this behavior.

In Figure 4 we plot x_e versus $n_{\text{H}_2}/\zeta_{-17}$, for five values of $k_{3,4}$, ranging from 0.2 to 5 times our standard 50 K value of $1.7 \times 10^{-7} \text{ cm}^3 \text{ s}^{-1}$. In these numerical computations, all other parameters, including all rate coefficients and gas-phase elemental abundances, are the same as in the computations we presented in §2. Figure 4 shows that for small $k_{3,4}$ bistability is suppressed, and that as $k_{3,4}$ is increased the gas becomes bistable for an increasing range of densities. For $n_{\text{H}_2}/\zeta_{-17}$ held fixed at, say, $1.0 \times 10^3 \text{ cm}^{-3}$, the gas is in the LIP or HIP for low or high $k_{3,4}$, and is bistable for intermediate values. This is the same behavior found by Pineau des Forets & Roueff (2000).

These results can be readily understood as follows. As the dissociative recombination rate coefficient of H_3^+ is increased, less O_2 is produced by the sequence (R6)-(R11) at any give density. An HIP can therefore be maintained to higher densities before O_2 becomes significant in removing S^+ . An increased H_3^+ recombination efficiency also implies that electrons become competitive with CO in removing H_3^+ at larger densities in the LIP. Quantitatively,

equation (11) shows that $(n_{\text{H}_2}/\zeta_{-17})_{\text{max}}$, the density above which O_2 begins removing S^+ , is proportional to $k_{3,4}^2$. However, $(n_{\text{H}_2}/\zeta_{-17})_{\text{min}}$, the density below which electrons begin removing the H_3^+ , varies only linearly with $k_{3,4}$. Therefore, as $k_{3,4}$ is reduced, $(n_{\text{H}_2}/\zeta_{-17})_{\text{max}}$ falls below $(n_{\text{H}_2}/\zeta_{-17})_{\text{min}}$, and bistability disappears. As $k_{3,4}$ is increased, $(n_{\text{H}_2}/\zeta_{-17})_{\text{max}}$ grows more rapidly, and eventually exceeds, $(n_{\text{H}_2}/\zeta_{-17})_{\text{min}}$, and the gas becomes bistable for an increasing range of densities. For example, if $k_{3,4}$ is increased by a factor of 5 relative to our standard value, Figure 4 shows that $(n_{\text{H}_2}/\zeta_{-17})_{\text{max}}$ increases by about a factor of 25, and $(n_{\text{H}_2}/\zeta_{-17})_{\text{min}}$ increases by about a factor of 5. This is consistent with expressions (11) and (18).

A similar scaling analysis may be carried out for the other parameters that control $(n_{\text{H}_2}/\zeta)_{\text{min}}$ and $(n_{\text{H}_2}/\zeta)_{\text{max}}$. For example, if the oxygen abundance is reduced our analysis shows that the regime of bistability should move to higher values of n_{H_2}/ζ , as found numerically by Viti et al. (2001) (see their Figures 5 and 7). For a lower oxygen abundance $(n_{\text{H}_2}/\zeta)_{\text{min}}$ is increased because the HIP can be maintained to a higher density before O_2 becomes abundant enough to remove the atomic ions. The reduced O_2 density leads to a higher electron density in the LIP, so $(n_{\text{H}_2}/\zeta)_{\text{min}}$ is increased as well.

Our numerical and analytic results show how the onset of the H_3^+ - O_2 - S^+ instability cycle depends on the O_2 and electron densities as determined by the elemental abundances and by the H_3^+ dissociative recombination rate coefficient. However, Figure 4 reveals an additional interesting feature. For $k_{3,4}$ equal to 0.2 times our standard value the gas again becomes marginally bistable at $(n_{\text{H}_2}/\zeta_{-17}) \approx 9 \text{ cm}^{-3}$. At such low densities the dominant atomic ion in the HIP is C^+ rather than S^+ (see Fig. 1). The instability, and the transition from HIP to LIP, is therefore modified by the addition of an identical H_3^+ - O_2 - C^+ cycle, with reactions (R19) and (R20) operating to neutralize the C^+ . The behavior in this numerical example is a bit more complicated because S^+ is still the dominant ion in the LIP at the transition density. We note that at such low densities realistic clouds would likely become “diffuse” and optically thin to external far-ultraviolet radiation, with a resulting reduction in O_2 and further modifications to the chemistry. We do not consider such effects here.

6. Gas-Grain Recombination

We have shown that bistability arises in purely gas-phase models, consistent with previous findings. When the HIP and LIP solutions “overlap”, neutralization of atomic ions (S^+ in our models) proceeds by either slow radiative recombination in the HIP, or via the formation of intermediate molecular ions ($\text{S}^+ + \text{O}_2 \rightarrow \text{SO}^+ + \text{O}$) followed by rapid dissociative recombination in the LIP. The two solutions are separated by a chemical instability, which

we have identified in our models as the $\text{H}_3^+ - \text{O}_2 - \text{S}^+$ cycle.

Our analysis suggests that bistability will be damped, or eliminated entirely, if additional neutralization processes are included that interrupt the $\text{H}_3^+ - \text{O}_2 - \text{S}^+$ cycle. We demonstrate this by considering how the single process of “grain assisted recombination” of atomic ions affects the chemistry. In this process, atomic ions recombine via electron transfer from grains to the ions during collisions with the grains (Draine & Sutin 1987; Weingartner & Draine 2001). The grain assisted recombination rate may be expressed as $k_g n_{\text{tot}}$, where n_{tot} is the total density of hydrogen nuclei. For any ion, k_g is an effective rate coefficient that depends on the dust-to-gas ratio, grain size distribution, grain charge, and gas temperature. This process dominates radiative recombination when $2k_g > k_r x_e$, where k_r is the radiative recombination rate coefficient. For $k_r \sim 10^{-11} \text{ cm}^3 \text{ s}^{-1}$ (appropriate for S^+), and a fractional ionization $x_e \approx 10^{-5}$, as occurs for densities near $(n_{\text{H}_2}/\zeta_{-17})_{\text{max}}$ in our computation (see Fig. 1), grain assisted recombination dominates radiative recombination for $k_g \gtrsim 5 \times 10^{-17} \text{ cm}^3 \text{ s}^{-1}$. This is well below the maximum values of $k_g \sim 10^{-14} \text{ cm}^3 \text{ s}^{-1}$ found by Weingartner & Draine, so this process is potentially relevant in determining the ionization balance. Furthermore, grain assisted recombination will interfere with the $\text{H}_3^+ - \text{O}_2 - \text{S}^+$ cycle and render it inoperative when $k_g > f_{\text{O}_2} X'_0 k_{22}$, where as previously defined, $f_{\text{O}_2} X'_0$ is the fraction of oxygen bound in O_2 , and $k_{22} = 1.5 \times 10^{-11} \text{ cm}^3 \text{ s}^{-1}$ is the rate coefficient of reaction (R22). For $f_{\text{O}_2} \approx 0.2$ and $X'_0 = 1.5 \times 10^{-4}$, the $\text{H}_3^+ - \text{O}_2 - \text{S}^+$ instability cycle is quenched when $k_d \gtrsim 5 \times 10^{-16} \text{ cm}^3 \text{ s}^{-1}$. Bistability and the sharp transition from HIP to LIP should then disappear.

We illustrate this in Figure 5, where we plot x_e versus $n_{\text{H}_2}/\zeta_{-17}$, for k_g ranging from zero (as in Figures 1 and 4) to $1.0 \times 10^{-14} \text{ cm}^3 \text{ s}^{-1}$, for all atomic ions. All other parameters are as in the calculation in §2. As k_g is increased the diminished electron density leads to more H_3^+ and O_2 in the HIP, so that $(n_{\text{H}_2}/\zeta_{-17})_{\text{max}}$ is reduced. Similarly, the onset of dissociative recombination in the LIP occurs at lower densities, and $(n_{\text{H}_2}/\zeta_{-17})_{\text{min}}$ is reduced. Thus, at first the bistability region shifts to lower densities as k_g is increased. However, as estimated above, when k_g exceeds $\sim 3 \times 10^{-16} \text{ cm}^3 \text{ s}^{-1}$ bistability is eliminated entirely, because the $\text{H}_3^+ - \text{O}_2 - \text{S}^+$ (and $\text{H}_3^+ - \text{O}_2 - \text{C}^+$) cycles are fully quenched, and neutralization occurs entirely by grain recombination.

These results strongly suggest that for realistic clouds, in which gas-grain neutralization is a likely important process, bistability will not occur. The precise value of k_g in dark clouds may be variable, as the grain population can be modified by coagulation (Draine 1985; Flower et al. 2005) and other processes. However, even with the removal of all grains with sizes below $\sim 15 \text{ \AA}$, the rate coefficient $k_g \sim 10^{-15} \text{ cm}^3 \text{ s}^{-1}$ (e.g. McKee 1989), which is sufficiently large to suppress bistability. We thus confirm and explain the results of Shalabiea and Greenberg (1995), who found that bistability is eliminated when gas-grain processes,

including grain assisted recombination, are incorporated in the numerical computations.

7. Summary

The non-linearity of equations (1)-(4) is a mathematical prerequisite for bistability and the appearance of multiple solutions (Le Bourlot et al. 1993, 1995; Lee et al. 1998; Pineau des Forets & Roueff 2000; Charnley & Markwick 2003). However, the purpose of our paper has been to identify and analyze the chemical mechanisms underlying the bistability phenomenon. We have shown that a simple chemical instability, involving atomic ions (typically S^+), O_2 molecules, and H_3^+ ions, allows multiple solutions to appear near the transition points from low-density high-ionization (HIP) to high-density low-ionization (LIP) conditions in the gas-phase chemistry. The instability drives the O_2 density to either small (HIP) or large (LIP) values. Bistability occurs when a low O_2 abundance in the HIP can be maintained up to maximal densities that are greater than the minimal densities above which a large O_2 density is maintained in the LIP. Two modes of neutralization are then simultaneously available to the gas. The slow (HIP) mode is radiative recombination (usually $S^+ + e \rightarrow S + \nu$). The fast (LIP) mode is formation of molecular ions followed by dissociative recombination (usually $S^+ + O_2 \rightarrow SO^+ + O$; $SO^+ + e \rightarrow S + O$).

We have derived simple analytic scaling relations for the range of gas densities and ionization rates for which bistability occurs. Our formulae show how the bistable range depends on the assumed gas-phase abundances, and several reaction rate-coefficients, including the dissociative recombination rate coefficient of H_3^+ . Bistability is eliminated when the two modes of gas-phase neutralization are superseded by gas-grain processes such as grain assisted recombination of the atomic ions. This likely happens for the range of electron and O_2 densities where bistability typically occurs in purely gas-phase models. We conclude that the bistability phenomenon probably does not occur in realistic dusty interstellar clouds, although it remains of theoretical interest.

Acknowledgments

We thank A. Dalgarno, O. Gnat, C.F. McKee, and D. Neufeld for discussions. We thank A. Markwick-Kemper for constructive comments on our manuscript. This research is supported by the Israel Science Foundation, grant 221/03.

REFERENCES

- Biham, O., & Lipshtat, A. 2002, *Phys. Rev. E*, 66, 056103
- Boger, G., & Sternberg, A. 2005, *ApJ*, 632, 302
- Cardelli, J.A., Mathis, J.S., Ebbets, D.C., & Savage, B.D. 1993, *ApJ*, 402, L17
- Cardelli, J.A., Sofia, U.J., Savage, B.D., Keenan, F.P., & Dufton, P.L. 1994, *ApJ*, 420, L29
- Charnley, S.B., & Markwick, A.J. 2003, *A&A*, 399, 583
- Draine, B.T. 1985, in *Protostars and Planets II*, ed. D. Black and M. Matthews (Tucson: University of Arizona Press), p. 33.
- Draine, B.T. & Sutin, B. 1987, *ApJ*, 320, 803
- Flower, D., Pineau des Forets, G., & Walmsley, C.M. 2005, *A&A*, 436, 933
- Gredel, R., Lepp, S., Dalgarno, A., & Herbst, E. 1989, *ApJ*, 347, 289
- Jensen, M.J., Bilodeau, R.C., Safvan, C.P., Seiersen, K., Andersen, L.H., Pedersen, H.B., & Heber, O. 2000, *ApJ*, 543, 764
- Le Bourlot, J., Pineau des Forets, G., Roueff, E., & Schilke, P. 1993, *ApJ*, 416, L87
- Le Bourlot, J., Pineau des Forets, G., Roueff, E., & Flower, D. R. 1995, *A&A*, 302, 870
- Le Bourlot, J., Pineau des Forets, G., & Roueff, E. 1995, *A&A*, 297, 251
- Lee, H.-H., Roueff, E., Pineau des Forets, G., Shalabiea, O. M., Terzieva, R., & Herbst, Eric 1998, *A&A*, 334, 1047
- Lepp, S., Dalgarno, A., van Dishoeck, E.F., & Black, J.H. 1988, *ApJ*, 329, 418
- Lepp, S., & Dalgarno, A. 1996, *A&A*, 306, L21
- Le Teuff, Y.H., Millar, T.J., & Markwick, A.J. 2000, *A&A*, 146, 157
1996, *ApJ*, 466, 561
- McCall, B.J. et al. 2004, *Phys.Rev.A*, 70, E2716
- McKee, C.F. 1989, *ApJ*, 345, 782
- Meyer, D.M., Cardelli, J.A., & Sofia, U.J. 1997, *ApJ*, 490, L103

- Meyer, D.M., Jura, M., & Cardelli, J.A. 1998, *AJ*, 493, 222
- Pineau des Forets, G., Roueff, E., & Flower, D.R. 1992, *MNRAS*, 258, 45
- Pineau des Forets, G., & Roueff, E. 2000, *Phil. Trans. R. Soc. Lond.*, 358, 2549
- Shalabiea, O.M. & Greenberg, J.M. 1995, *A&A*, 296, 779
- Sternberg, A., Dalgarno, A., & Lepp, S. 1987, *ApJ*, 320, 676
- Sternberg, A., & Dalgarno, A. 1995, *ApJS*, 99, 565
- Vidali, G., Roser, J.E., Manic, G., & Pirronello, V. 2004, *JGR*, 109, E7, E10907S14
- Viti, S., Roueff, E., Hartquist, T.W., Pineau des Forts, G., Williams, D.A. 2001, *A&A*, 370, 557
- Weingartner, J.C., & Draine, B.T. 2001, *ApJ*, 563, 842

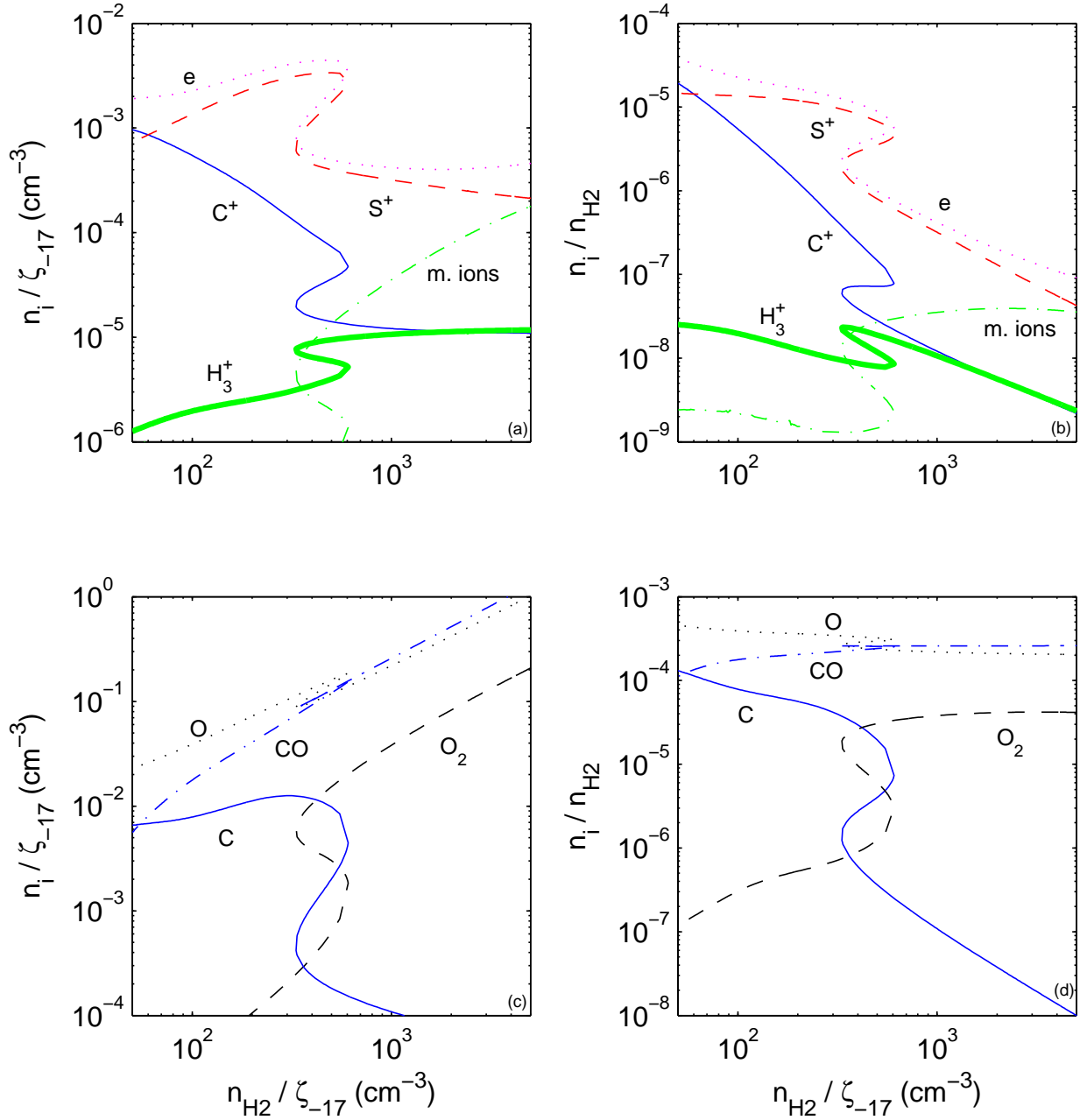


Fig. 1.— The steady-state densities n_i/ζ_{-17} , and density fractions n_i/n_{H_2} , of electrons, S^+ , C^+ , and H_3^+ ions, C, and O atoms, and CO and O_2 molecules, as functions of $n_{\text{H}_2}/\zeta_{-17}$. An HIP exists for densities less than 675 cm^{-3} , and a LIP exists for densities greater than 370 cm^{-3} . The gas is bistable between these densities.

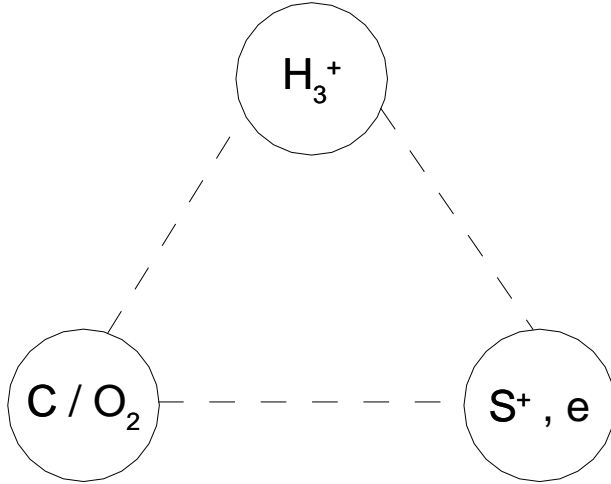


Fig. 2.— The $H_3^+ - O_2 - S^+$ cycle. Increasing the electron density, reduces H_3^+ via dissociative recombination. This reduces O_2 formed by the sequence (R6)-(R11). Destruction of S^+ by O_2 decreases, so the S^+ density increases. This cycle can “run away” when S^+ is the dominant positive charge carrier (see text).

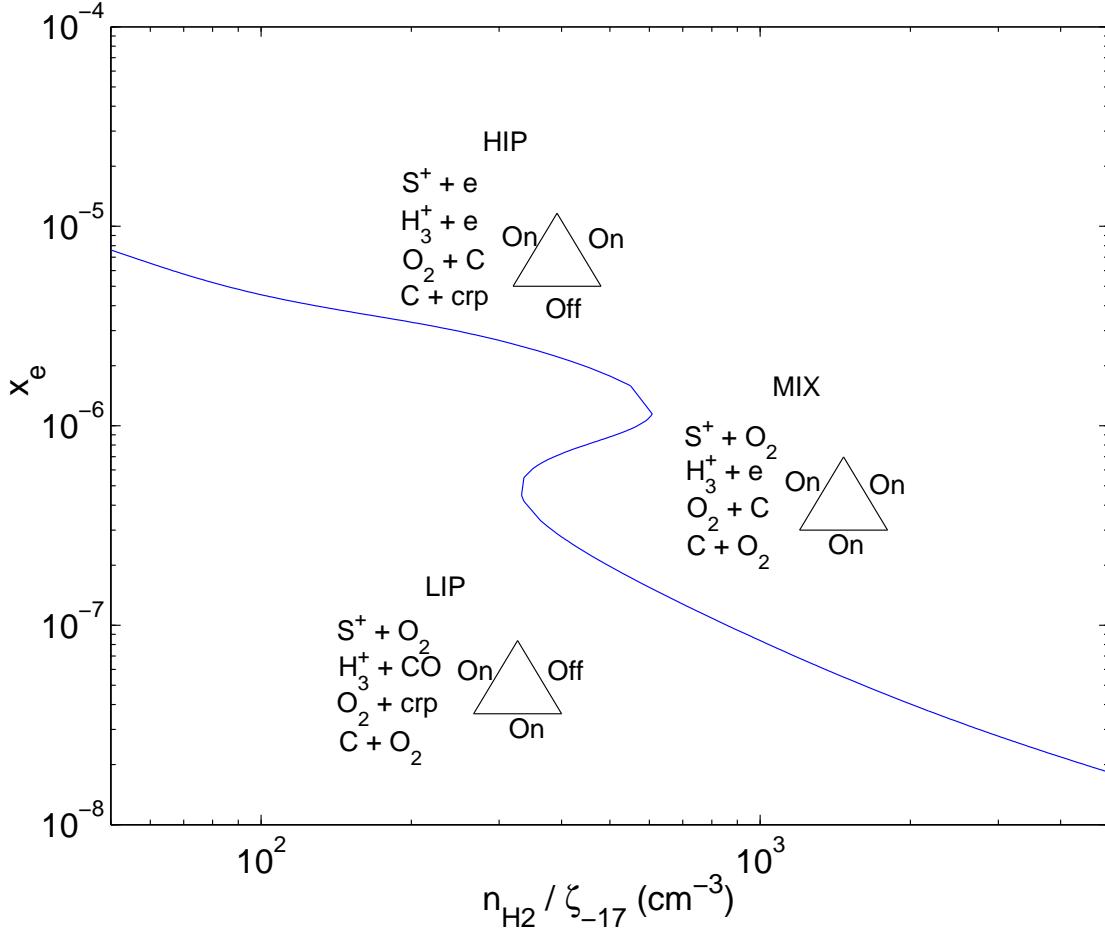


Fig. 3.— The fractional ionization, $x_e \equiv n(e)/n_{\text{H}_2}$, versus $n_{\text{H}_2}/\zeta_{-17}$, for our standard model. The dominant destruction reactions for S^+ , H_3^+ , O_2 , and C , are indicated for each of the three HIP, MIX, and LIP branches in the bistability region. E.g., “ $\text{S}^+ + e$ ” indicates that S^+ is removed by recombination with electrons. The triangles indicate which “legs” of the $\text{H}_3^+ - \text{O}_2 - \text{S}^+$ instability cycle operate in each of the three phases.

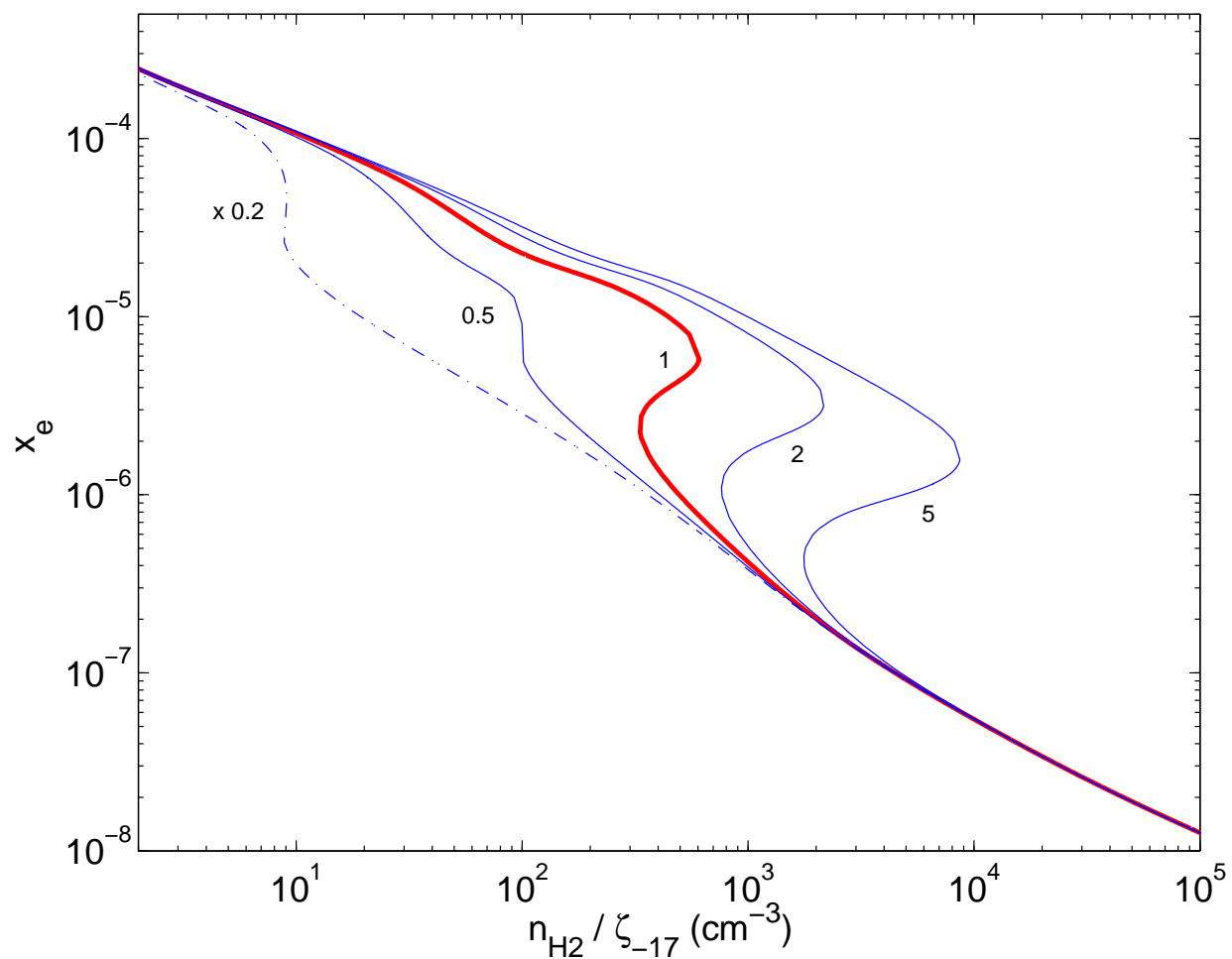


Fig. 4.— The fractional ionization, $x_e \equiv n_e/n_{\text{H}_2}$, for five values of the H_3^+ dissociative recombination rate coefficient $k_{3,4}$, ranging from 0.2 to 5 times our standard value of $1.7 \times 10^{-7} \text{ cm}^3 \text{ s}^{-1}$. For the lowest value of $k_{3,4}$ (dot-dashed curve) C^+ rather than S^+ is the dominant positive ion near the transition point in the HIP (see text).

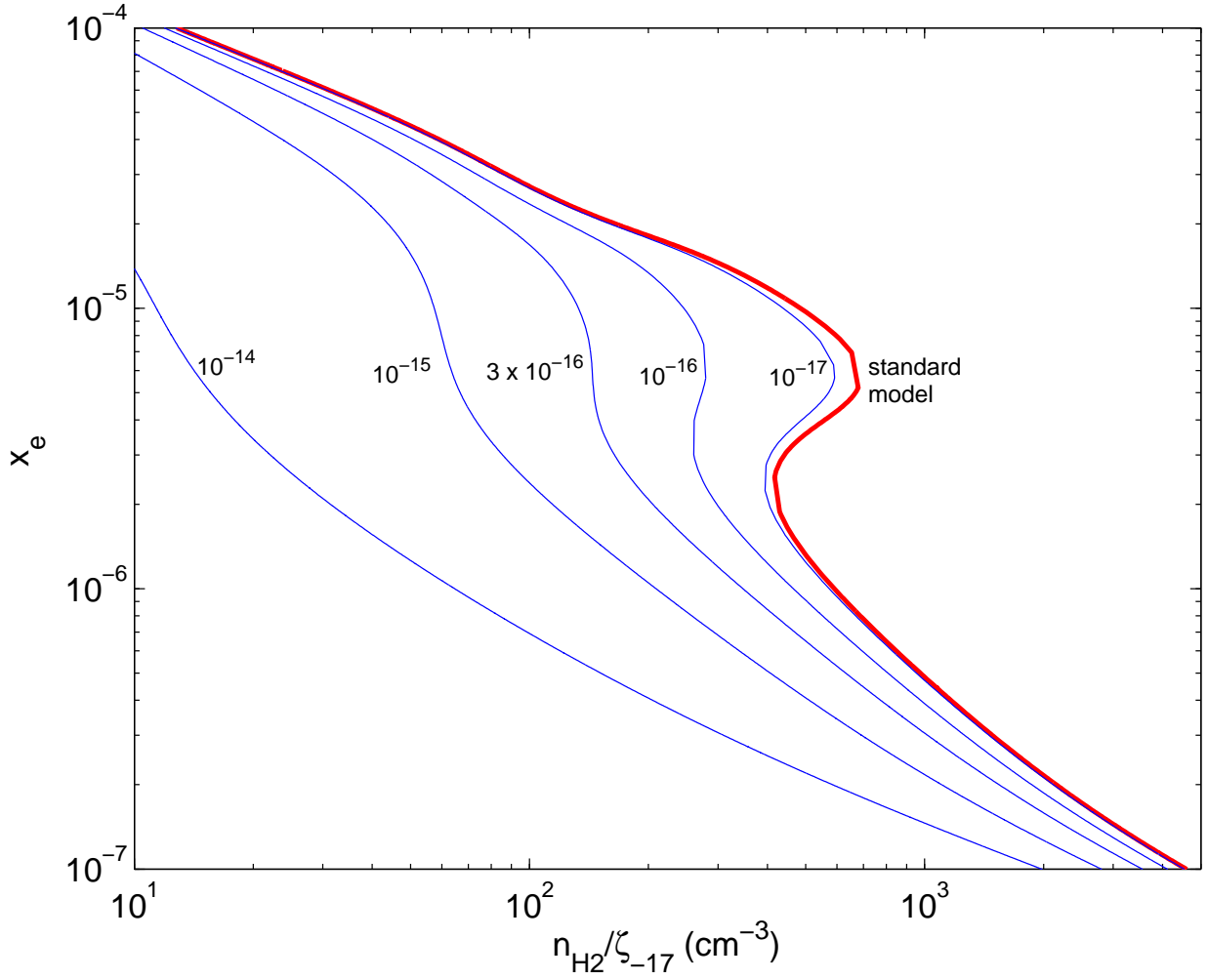


Fig. 5.— The fractional ionization for grain-assisted recombination rate-coefficients for all atomic ions varying from $k_g = 1.0 \times 10^{-17}$ to $1.0 \times 10^{-14} \text{ cm}^3 \text{ s}^{-1}$. For our standard model, $k_g = 0$.

Table 1. Atomic and molecular densities, and density ratios.

	HIP	MIX	LIP	ratio
H	1.7(-1)	1.7(-1)	1.7(-1)	1.0
H ₂	4.3(2)	4.3(2)	4.3(2)	1.0
C	1.1(-2)	1.3(-3)	2.2(-4)	50.0
N	2.8(-2)	1.9(-2)	1.0(-2)	2.8
O	1.4(-1)	1.2(-1)	1.0(-1)	1.4
S	2.6(-3)	3.8(-3)	3.6(-3)	0.72
Si	2.1(-5)	2.9(-5)	2.7(-5)	0.78
e	4.4(-3)	1.7(-3)	5.3(-4)	8.30
C ⁺	9.0(-5)	3.1(-5)	1.5(-5)	6.0
N ⁺	5.0(-10)	5.4(-10)	6.0(-10)	0.83
O ⁺	4.2(-11)	1.1(-10)	1.9(-10)	0.22
S ⁺	3.3(-3)	1.3(-3)	4.3(-4)	7.67
Si ⁺	9.8(-4)	2.7(-4)	6.1(-5)	16.1
H ₃ ⁺	3.6(-6)	6.3(-6)	9.0(-6)	0.40
H ₃ O ⁺	9.6(-8)	4.4(-7)	1.9(-6)	0.051
HCO ⁺	2.3(-7)	1.2(-6)	5.2(-6)	0.044
HCS ⁺	7.3(-8)	2.1(-7)	9.6(-7)	0.076
CO ⁺	2.2(-11)	5.8(-11)	9.5(-11)	0.23
NO ⁺	1.1(-8)	4.6(-8)	1.2(-7)	0.092
O ₂ ⁺	2.5(-9)	2.8(-8)	1.9(-7)	0.013
SO ⁺	3.7(-8)	1.6(-7)	5.2(-7)	0.071
CH	2.7(-6)	7.3(-7)	3.0(-7)	9.0
NH	1.1(-6)	1.5(-6)	2.0(-6)	0.55
OH	2.8(-5)	6.3(-5)	1.1(-4)	0.25
H ₂ O	2.8(-4)	1.1(-3)	2.1(-3)	0.13
SH	3.9(-7)	6.1(-7)	1.0(-6)	0.39
SiH	1.6(-7)	5.0(-8)	1.2(-8)	13.3
CO	1.0(-1)	1.1(-1)	1.1(-1)	0.91
NO	3.0(-5)	1.2(-4)	3.0(-4)	0.1
O ₂	4.2(-4)	3.6(-3)	1.2(-2)	0.035
SO	6.5(-6)	1.2(-4)	8.0(-4)	0.008
SiO	5.3(-4)	1.2(-3)	1.4(-3)	0.38
CS	1.2(-3)	1.8(-3)	2.2(-3)	0.55
CN	4.5(-6)	2.0(-6)	1.3(-6)	3.46
HCN	4.6(-5)	1.0(-5)	3.2(-6)	14.4
N ₂	1.8(-2)	2.2(-2)	2.7(-2)	0.67

Note. — Densities (cm^{-3}) of selected species, for the three HIP, MIX, and LIP solutions, for $n_{\text{H}_2} = 4.3 \times 10^2 \text{ cm}^{-3}$, and $\zeta = 1.0 \times 10^{-17} \text{ s}^{-1}$. Column 5 lists HIP/LIP density ratios.